



Lasers in Manufacturing Conference 2015

Simulation of Laser Welding of Dissimilar Metals

Rodrigo Gómez Vázquez*, Andreas Otto, Gerhard Liedl, and Robert Feichtenschlager

Institute for Production and Laser Technology, Vienna University of Technology, Getreidemarkt 9, 1060 Vienna, Austria

Abstract

Welding of dissimilar metals in general is a complicated task that involves many difficulties. Currently one of the most challenging problems is the formation of inter-metallic phases in the joining interface. In this paper we introduce a simulation model aimed to support the study of laser dissimilar welding by providing useful information on the process characteristics (e.g. thermal distribution, species mixing) including inter-metallics formation. The introduced model is based on our existing multi-physical solver for simulation of laser processes within OpenFOAM's environment. The simulation capabilities were extended with new physics for the study of dissimilar welding processes. Multi-species diffusion and a simplified growth model for the intermetallic layer were included. Implemented diffusion includes temperature dependency and allows simultaneous mixing of different species. The formation of inter-metallic phases is calculated by a species reaction model coupled with both species and energy transport models. The thickness of the inter-metallic layer predicted by the simulations is finally compared with experimental data for aluminum and steel.

Keywords: multi-physical simulation; laser welding; dissimilar materials; inter-metallic phases.

1. Introduction

Increasing industrial demand of hybrid components enhances the interest on the fabrication of dissimilar metal joints by laser assisted techniques. However, the laser welding of dissimilar materials usually results in a challenging task, due to the complex material interactions and the current lack of knowledge about the inner process mechanisms. Dissimilar laser welding has been extensively studied over the last decades by means of empirical methods. Fortunately nowadays the available computational power allows numerical assisted

* Corresponding author. Tel.: +43-1-58801-311626; fax: +43-1-58801-9311611.
E-mail address: rodrigo.gomez.vazquez@tuwien.ac.at

investigations as well. Most of the numerical studies on dissimilar laser welding were aimed to provide reference thermal profiles e.g. [1]. Up to the date we could only find a few works including the effects of the melt pool dynamics in their results [2 to 11].

In this paper we present an extended multi-physical model capable to simulate the whole process in a macro- and meso-scale,comprehending from the melt pool dynamics up to the formation of inter-metallic compounds. The model has been developed with the aim of serving as support for further investigations on the field of laser assisted dissimilar welding.

2. Simulation model

The simulation model is based on our multi-physical model for laser assisted processing developed within an OpenFOAM® environment. Extended descriptions of the model can be found in [12 to 14]. Presented model developments suppose the continuation of the work first described in [15]. New implementations are described below:

2.1. Multi-species diffusion

The module is based on Fick's diffusion laws. Diffusion coefficients are modelled as temperature-dependent Arrhenius functions according to:

$$D=D_0*\exp(-Q/R/T) \quad (1)$$

,where D_0 is the pre-exponential diffusion factor, Q is the activation energy for the diffusion, R is the universal gas constant and T is the absolute temperature. We use an iterative approach that is capable to evaluate diffusion of multiple phases into each other simultaneously. This requires the use of a more advanced treatment for the phase field. Due to the VOF-nature of the multi-phase model used it is possible that several species find themselves sharing a same mesh element, whose properties will be averaged. In some cases two condensed diffusing species have to share the volume element with an overheated species, leading to a mean element temperature well beyond the temperature range at which those condensed species can be expected. In such cases, simply following the Arrhenius function for the diffusion coefficient would lead to unrealistic diffusion coefficients. An artificial limitation of those coefficients beyond their temperature range has been included to avoid such issues. Due to the new functionality brought in by the subsequently described reaction model decision variables had to be introduced in the solver to switch to the inter-diffusion coefficient through the inter-metallic phase once it is already present in a certain mesh element.

2.2. Reaction model

The model takes into account the temperature and the concentration of the different reacting species present in each mesh element to allow their recombination to create an inter-metallic compound according to a given stoichiometric relation. Currently, the model only accepts a single inter-metallic phase, although its extension to deal with multiple inter-metallic phases is planned. Since most of this reactions are exothermal, no activation energy has been implemented. However a minimal temperature for the reaction to take place can be specified. In addition, an energy source term has been included to take into account the energy release produced by the reaction. Its integration into the thermal calculation is similar to one arising from the source term due to the absorption of the laser power.

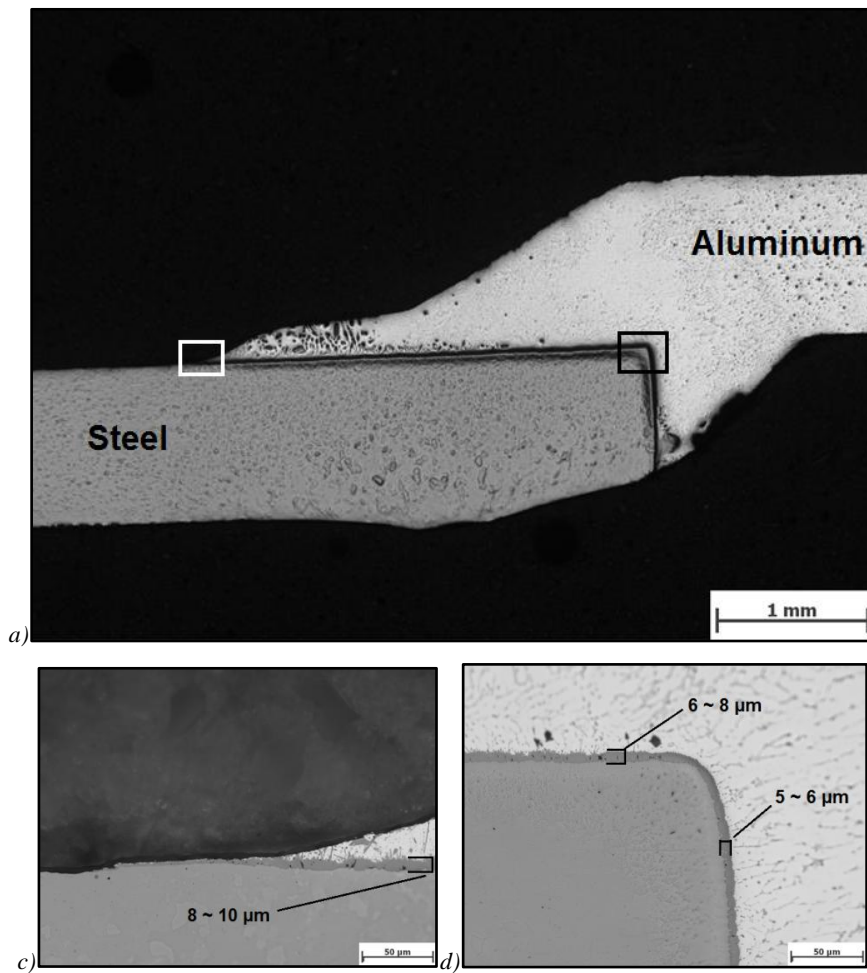


Fig. 1. (a) Cross section of the weld joint (laser light comes from the bottom) [17]; (b) thickness of the inter-metallic layer at the wetting front [17]; (c) thickness of the inter-metallic layer at the corner [17].

3. Application to a real process: aluminum-steel welding

In order to test the capabilities of the multi-physical model with the new developments we made use of available experimental results from older projects [16, 17]. More precisely, the process chosen was laser beam welding of aluminum and steel in overlap configuration.

In a first instance, we reproduced the macroscopic features e.g. wetting by means of 2D and 3D process simulations. After that, we made use of 2D simulations to obtain an estimation of the thickness of the inter-metallic layer.

3.1. Experimental conditions

Joining of sheets of a low-alloyed steel (DC01) with a weldable AlMgSi aluminum-alloy (AW6016) has been chosen. Materials thickness was 1mm for both steel and aluminum plates. The sample has been welded in an overlap configuration with an overlap factor of 1.5 mm. A 3 kW lamp pumped Nd:YAG laser guided by means of a 600 μm fiber was used. The laser radiation was focused by a lens with a focal length of 250 mm. Lateral alignment of the focal spot of the laser has been kept constant at a distance of 0.5 mm measured from the edge of the sample and the axial focal position was 40 mm above the steel plate. Line energy was 107 J/mm. Shielding gas (argon) was used, as well as flux. Figure 1 shows the cross section of the weld joint.

3.2. Simulation of the macroscopic features

According to the Al-Si phase diagram, even the small amount of silicon present in the 6016 alloy (1.0 to 1.5%) is enough to create a mushy region for a range of 50 to 60 K below the liquidus line. Though it was not possible to achieve a numerically stable implementation of the viscosity change due to the mushy region in the simulation in the course of this study, the main process characteristics could be successfully reproduced.

Figure 2 shows the different stages of the process for an exemplary cross section. The energy of the process comes mainly from the absorption of the laser light by the steel plate. The amount directly absorbed by the aluminum plate also contributes to heat up the aluminum at the beginning but it does not play any relevant role compared to the direct heat conduction. Note that the isothermal lines reach first the other side of the steel plate right at the end of the aluminum plate, which is the closest point where the steel surface does not have an enhanced heat removal. Indeed this is the point where aluminum starts to melt. At this point the surface of the steel began already to melt too. As the melting front advances into the aluminum plate, wetting starts to show up at the other side. When the melting front reaches the edge of the steel plate, a second wetting along the edge commences. This secondary wetting, which manifests as an increased contact interface, provides a much more efficient heat removal from the steel plate.

Once the laser and the plates begin to cool down aluminum starts to solidify. Two confronting solidification fronts can be identified. Each of them imposes a different angle to the free surface. When the warmest region solidifies both fronts join and leave an inflection point in the inclination trend of the free surface. As shown in Figure 1, this effect can be seen in the experimental sample under the same conditions. It must be accentuated that without considering any effect due to the welding flux nor due to oxidation of the surfaces the final length of the wetting achieved by the simulations is about 3mm, which is consistent with the experimental results.

Figure 3 shows the process in a 3D simulation. An evident asymmetry in the thermal distribution can be perceived, especially at the bottom side, where the main wetting process takes place. From the picture one can notice that the actual phenomenon is more complex than the exposed in the 2D-case, since it spreads forwards and backwards too, contributing to spread the heat. The secondary wetting along the edge is also significant. In some of the experiments cooling plates of different materials e.g. copper were used to enhance the cooling of the aluminium plate. The problem of the excess of heat can be noticed from the pictures too.

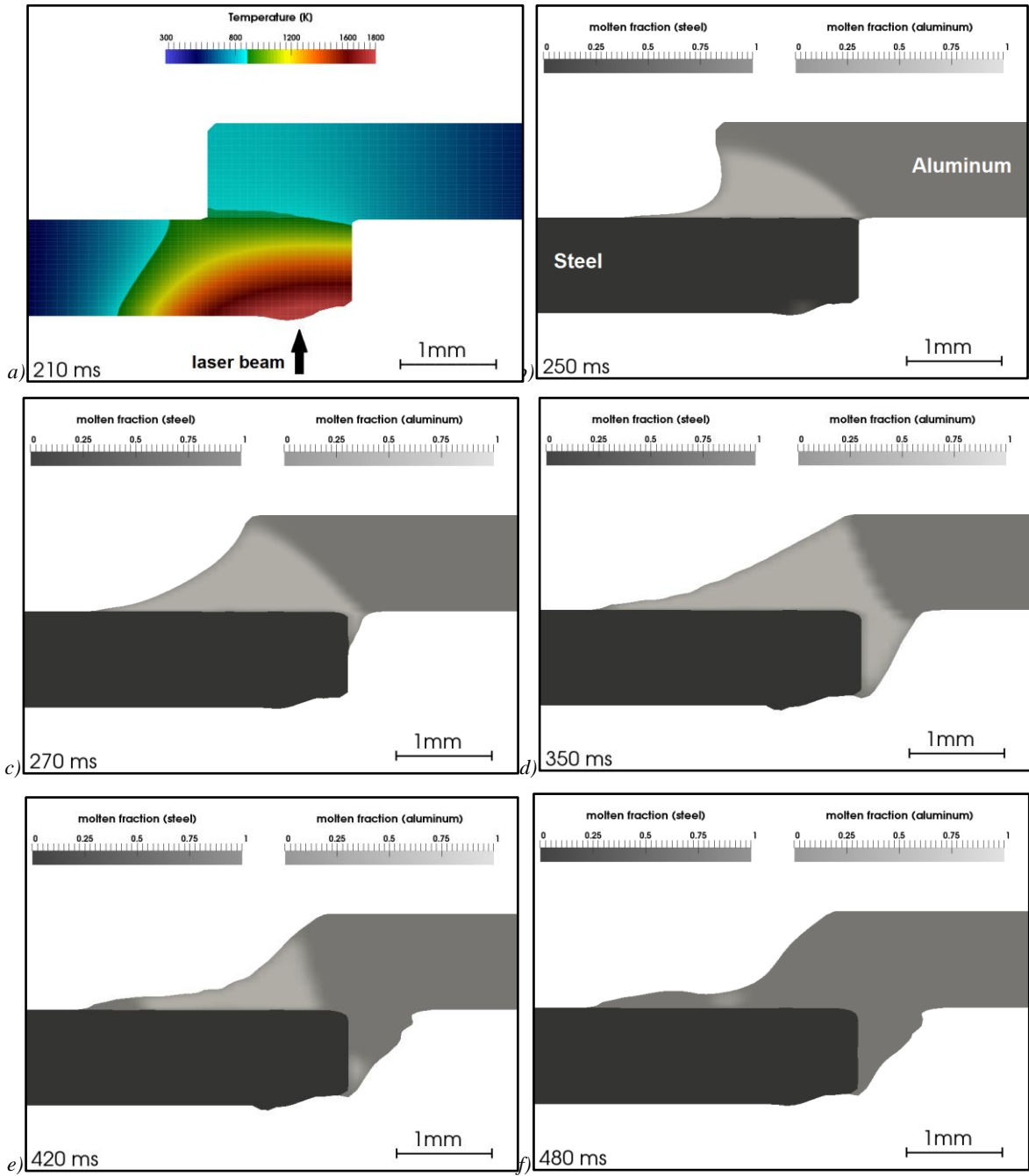


Fig. 2. Evolution of the joining process step by step for a cross section. (a) thermal profile (the arrow indicates the incidence of the light); (b) to (f) molten fractions of the metals.

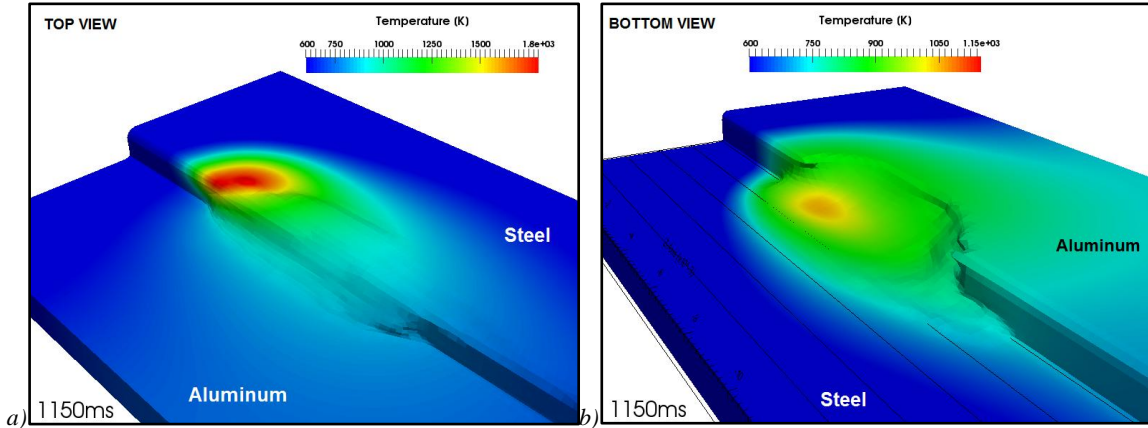


Fig. 3. 3D-Simulation of the overlap laser welding of aluminum and steel.(a) View from the top; (b) Bottom view showing the evolution of the wetting.

3.3. Growth of the inter-metallic layer

The advantage of laser wetting is that the process can be performed within temperatures not much higher than the melting point of the aluminum. Mixing of both metals in liquid state can be avoided and therefore the diffusion is limited. At the region where the steel is in contact with the aluminum the diffusion of solid iron into liquid aluminum takes place much faster than vice-versa [1]. According to the phase diagram iron-aluminum, a solution with high concentration of aluminum at temperatures slightly above the melting should only promote formation of FeAl_3 . However, according to the literature Fe_2Al_5 grows much faster than FeAl_3 in the initial stages [18]. Indeed, the growth of Fe_2Al_5 has been described as parabolic, while FeAl_3 follows a linear growth function [19]. Therefore in this study we suppose the formation of Fe_2Al_5 as only inter-metallic phase.

Our intention was to reproduce the growth of the inter-metallic phases via their inter-diffusion coefficients. Unfortunately it is not easy to find reliable values to use as input for our model. There is much more work performed for long-time diffusion of Fe-Al than for short time e.g. [20]. Works dealing with shorter time scales mostly try to obtain the growth kinetic constants of the inter-metallics from the correlation of the thickness with the time [19, 21, 22]. There is a certain variability of the data, depending on the minimum studied time. The shortest time-scale study found was has been performed by [21]. From the kinetic growth constant for Fe_2Al_5 a diffusion coefficient of $2.16 \times 10^{-10} \text{m}^2/\text{s}$ for a constant temperature of 1073K was obtained. In absence of more precise data we had set this value as non-temperature dependent. Diffusion between aluminum and the inter-metallic phase was neglected, because it shall be implicitly included in the coefficient deduced from the growth kinetics for Fe_2Al_5 . Other diffusion coefficients taken are $D_0 = 26.79 \text{m}^2/\text{s}$ and $Q = 247 \text{kJ/mol}$ for solid Fe in solid Al [23] and $D_0 = 3.7 \times 10^{-7} \text{m}^2/\text{s}$ and $Q = 38.9 \text{kJ/mol}$ for Fe solid in liquid Al respectively [24]. The energy source term used due to the formation of inter-metallics was $2 \times 10^5 \text{J/mol}$ [25].

Figure 4 shows the inter-metallic layer predicted by the simulations. The thickness of this layer can be deduced from the volume fraction of the inter-metallic phase. Away from the corners we can consider homogeneous transversal growth. In that case, we can expect the phase to be gradually filling the cells from the interface outwards, thus its volume fraction multiplied by the transversal cell dimension gives the layer thickness. In the Figure 4 c) the cells at the interface have a width of $83 \mu\text{m}$ and a height of $28 \mu\text{m}$. According

to the phase level shown, predicted layer is less than $8\mu\text{m}$ at the top and less than $3\mu\text{m}$ at the right-hand side. Similarly, the predicted layer at the wetting front, in Figure 4 b), is less than $5\mu\text{m}$ thick. Numerical problems arising in the phase gradient scheme used for the species diffusion model avoided us to obtain reliable results with a finer mesh resolution. Nevertheless, these values are in reasonable agreement with the experimental results.

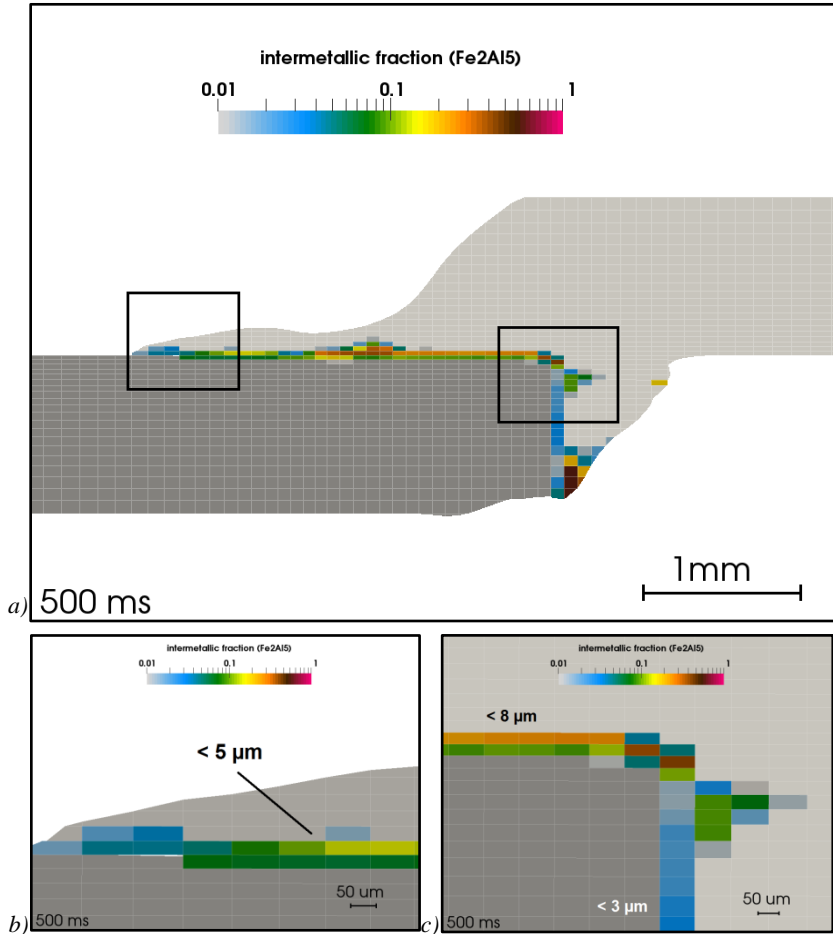


Fig. 4. (a) Simulated cross section showing the calculated distribution of inter-metallic phase; (b) Detail of the inter-metallic fraction at the wetting front; (c) Detail of the inter-metallic fraction at the corner.

4. Summary and Outlook

By extending the capabilities of a multi-physical model for laser material processing it has been possible to simulate the welding of a complex dissimilar metal couple such as aluminum and steel. Despite of the numerical problems and the simplification assumptions up to our knowledge this is the firsttime that a laser dissimilar welding process can be simulatedreproducing at the same time both macroscopic features such as the wetting phenomenon and microscopic features such as the growth of the inter-metallics. The model used for this study is at the same time being used with reasonable success for the simulation of other different

processes namely laser assisted ablation, laser assisted cutting and deep penetration welding among others. Further development aimed to the study of dissimilar welding includes the formation of different inter-metallic phases and thermal-induced stress fields.

References

- [1] Peyre, P., Sierra, G., Deschaux-Beaume, F., Stuart, D., Fras, G., 2007. Generation of aluminium–steel joints with laser-induced reactive wetting, *Materials Science and Engineering: A*, Volume 444, Issues 1–2, 25 January 2007, Pages 327–338
- [2] F. K. Chung, P. S. Wei, 1999. Mass, Momentum, and Energy Transport in a Molten Pool When Welding Dissimilar Metals. *ASME. J. Heat Transfer*. 1999;121(2):451-461 s
- [3] P. S. Wei, F. K. Chung, 2000. Unsteady marangoni flow in a molten pool when welding dissimilar metals, *Metallurgical and Materials Transactions B*, December 2000, Volume 31, Issue 6, pp 1387-1403
- [4] G. Phanikumar, K. Chattopadhyay, Pradip Dutta, 2001. Modelling of transport phenomena in laser welding of dissimilar metals, *International Journal of Numerical Methods for Heat & Fluid Flow*, 2001, 11:2, 156-174
- [5] Gandham Phanikumar, Kamanio Chattopadhyay, Pradip Dutta, 2004. Computational modeling of laser welding of Cu-Ni dissimilar couple, *Metallurgical and Materials Transactions B*, April 2004, Volume 35, Issue 2, pp 339-350
- [6] Nilanjan Chakraborty, 2009. The effects of turbulence on molten pool transport during melting and solidification processes in continuous conduction mode laser welding of copper–nickel dissimilar couple, *Applied Thermal Engineering* 29 (2009) 3618–3631
- [7] Nilanjan Chakraborty, Suman Chakraborty, 2007. Modelling of turbulent molten pool convection in laser welding of a copper–nickel dissimilar couple, *International Journal of Heat and Mass Transfer* 50 (2007) 1805–1822
- [8] S. Mukherjee, S. Chakraborty, R. Galun, Y. Estrin, I. Manna, 2010. Transport phenomena in conduction mode laser beam welding of Fe–Al dissimilar couple with Ta diffusion barrier, *International Journal of Heat and Mass Transfer* 53 (2010) 5274–5282
- [9] I. Tomashchuk, J.-M. Jouvard, P. Sallamand, 2007. Numerical modeling of copper-steel laser joining, Excerpt from the Proceedings of the COMSOL Users Conference 2007 Grenoble
- [10] I. Tomashchuk*, P. Sallamand, J.M. Jouvard, D. Grevey, 2010. The simulation of morphology of dissimilar copper–steel electron beam weld using level set method, *Computational Materials Science* 48 (2010) 827–836
- [11] Yaowu Hu, Xiuli He, Gang Yu, Zhifu Ge, Caiyun Zheng, Weijian Ning, 2012. Heat and mass transfer in laser dissimilar welding of stainless steel and nickel, *Applied Surface Science*, Volume 258, Issue 15, 15 May 2012, Pages 5914-5922
- [12] Koch, H., Gómez Vázquez, R., Otto, A., 2012. A Multiphysical Simulation Model for Laser Based Manufacturing, *Proceedings of the 6th European Congress on Computational Methods in Applied Sciences and Engineering – ECOMASS 2012*, 4546
- [13] Otto, A., Koch, H., Gómez Vázquez, R., 2012. Multiphysical simulation of laser material processing. *Proceedings of the 7th International Conference on Photonic Technologies LANE 2012*, *Physics Procedia* 39, 843-852
- [14] Andreas Otto, Holger Koch, Rodrigo Gómez Vázquez, Zhibin Lin, Bob Hainsey, 2014. Multiphysical Simulation of ns-Laser Ablation of Multi-material LED-structures, *Physics Procedia*, Volume 56, 2014, Pages 1315-1324
- [15] Gómez Vázquez, R., Koch, H.M., Otto, A., 2014. Multi-physical Simulation of Laser Welding, *Physics Procedia*, Volume 56, 2014, Pages 1334-1342
- [16] Liedl, G., Bielak, R., Ivanova, J., Enzinger, N., Figner, G., Bruckner, J., Pasic, H., Pudar, M., Hampel, S., 2011. Joining of Aluminum and Steel in Car Body Manufacturing, *Physics Procedia*, Volume 12, Part A, 2011, Pages 150-156
- [17] Mayr, M., 2010. Untersuchung des intermetallischen Phasenwachstums von lasergeschweißten Stahl-Aluminium Verbindungen, Master Thesis, Vienna University of Technology
- [18] Sina, H., Corneliussen, J., Turba, K., Iyengar, S., 2015. A study on the formation of iron aluminide (FeAl) from elemental powders, *Journal of Alloys and Compounds*, Volume 636, 5 July 2015, Pages 261-269
- [19] Bouayad, A., Gerometta, Ch., Belkebir, A., Ambari, A., 2003. Kinetic interactions between solid iron and molten aluminium, *Materials Science and Engineering: A*, Volume 363, Issues 1–2, 20 December 2003, Pages 53-61.
- [20] Jindal, V., Srivastava, V.C., 2008. Growth of intermetallic layer at roll bonded IF-steel/aluminum interface, *Journal of Materials Processing Technology*, Volume 195, Issues 1–3, 1 January 2008, Pages 88-93
- [21] Bouché, K., Barbier, F., Coulet, A., 1998. Intermetallic compound layer growth between solid iron and molten aluminium, *Materials Science and Engineering: A*, Volume 249, Issues 1–2, 30 June 1998, Pages 167-175
- [22] Novák, P., Michalčová, A., Marek, I., Mudrová, M., Saksli, K., Bednarčík, J., Zikmund, P., Vojtěch, D., 2013. On the formation of intermetallics in Fe–Al system – An in situ XRD study, *Intermetallics*, Volume 32, January 2013, Pages 127-136
- [24] Yong Du, Y.A Chang, Baiyun Huang, Weiping Gong, Zhanpeng Jin, Honghui Xu, Zhaohui Yuan, Yong Liu, Yuehui He, F.-Y Xie, 2003. Diffusion coefficients of some solutes in fcc and liquid Al: critical evaluation and correlation, *Materials Science and Engineering: A*, Volume 363, Issues 1–2, 20 December 2003, Pages 140-151.
- [23] Paul Heitjans, Jörg Kärger, 2006. *Diffusion in Condensed Matter. Methods, Materials, Models*, Ed. Springer, p.39.
- [24] Shahverdi, H.R., Ghomashchi, M.R., Shabestari, S., Hejazi, J., 2002. Microstructural analysis of interfacial reaction between molten aluminium and solid iron, *Journal of Materials Processing Technology*, Volume 124, Issue 3, 20 June 2002, Pages 345-352